IEICE TRANS. COMMUN., VOL.E88–B, NO.6 JUNE 2005

PAPER Special Section on 2004 International Symposium on Antennas and Propagation

Simultaneous Measurement of Antenna Gain and Solution Dielectric Properties

Nozomu ISHII[†a)], ***Member***, **Yoshikazu YONEMURA**[††], ***Student Member***, ***and*** **Michio MIYAKAWA**[†], ***Member***

SUMMARY A method is presented for the simultaneous measurement of the absolute gain of antennas in solution and the dielectric properties of the solution. The principle and formulation are based on a modified Friis transmission formula. This three-antenna method is applied to gain measurement of printed dipole antennas in solution, and demonstrated through comparison with calculated results to be an accurate method for the measurement of both antenna gain and solution dielectric properties.

key words: *absolute gain, solution, Friis transmission formula, three-antenna method, dielectric properties*

1. Introduction

Chirp-pulse microwave computed tomography (CP-MCT) is a three-dimensional thermometry technique that has been developed for non-invasive biological imaging for over 20 years [1]–[5]. In this technique, the spatial distribution of complex permittivity in a living body is measured by repeated translational and rotational scans. Then, as the complex permittivity of biological tissue is temperature-dependent at microwave frequencies [4], the temperature variation in the body can be obtained. In practice, biological objects are immersed in a solution with dielectric properties approximately equivalent to those of the living body to suppress reflections from the object surface. The influence of both diffraction from the object and reflection from the walls of the tank can be ignored because of the large attenuation in solution at microwave frequencies. A fan beam-type CP-MCT technique has been developed to speed up the imaging process, in which many antenna elements are installed to receive the microwave signal [5].

Many types of antenna can be employed for fan-beam detection in solution including an insulated dipole [6], a microstrip antenna [7], and a dielectric-loaded open waveguide [4], and the absolute gain such antennas in a dissipative medium has also been theoretically discussed [8], [9]. The present study considers an antenna array fabricated by printing the antennas on a substrate, which allows for the precise arrangement of elements along an arc at equal intervals [5].

One-step calibration of the probe in the specific absorption rate (SAR) dosimetric assessment system is an example of the use of two antennas for determining the absolute gain in solution [10]. In that method, two identical antennas are located so as to satisfy the far-field condition, and the gains are evaluated using the modified Friis transmission formula in lossy media. Methods such as the contact probe [11], slotted line [12], and TEM-line [13] techniques are often used to measure dielectric parameters.

In this study, a method for measuring the absolute gain and dielectric properties of the solution by a three-antenna method is discussed for the first time. The proposed method provides a one-step, simultaneous measurement of the absolute gain and dielectric parameters of the solution minimizing error in the measured dielectric parameters, and also introduces a technique of moving the antenna through the solution and applying curve fitting to reduce noise due to the solution. This paper presents the principle and formulation of the simultaneous measurement of absolute gain and dielectric properties (dielectric constant and conductivity) of the solution, which are based on a modified Friis transmission formula. The measurement setup and conditions for gain measurement of printed antennas in solution are described, and measurement results of the absolute gain and dielectric properties are shown to verify the effectiveness of the proposed method.

2. Principle of Measurement

2.1 Definition of Antenna Gain in Dissipative Media

The absolute gain of an antenna in a dissipative medium is as follows. According to [9], the power radiated from an antenna can be defined in two ways:

1. Radiated power can be estimated in the far-field zone [8] by

$$P_{\mathrm{rad}} = e^{2\alpha r} \iint_S \mathrm{Re}\left[\frac{1}{2}\mathbf{E}\times\mathbf{H}^*\right]\cdot d\mathbf{s}, \tag{1}$$

where $\mathbf{E}$ and $\mathbf{H}$ are field vectors on the surface S which is a spherical surface with radius r from the center of the antenna, and α is the attenuation constant of the medium. The superscript $*$ denotes the conjugate of the complex number.

2. Alternatively, radiated power can be estimated in close vicinity to the antenna by

$$P'_{\mathrm{rad}} = \iint_{S'} \mathrm{Re}\left[\frac{1}{2}\mathbf{E}\times\mathbf{H}^*\right]\cdot d\mathbf{s}, \tag{2}$$

Manuscript received October 1, 2004.
Manuscript revised January 12, 2005.

[†]The authors are with the Department of Biocybernetics, Faculty of Engineering, Niigata University, Niigata-shi, 950-2181 Japan.
[††]The author is with the Graduate School of Science and Technology, Niigata University, Niigata-shi, 950-2181 Japan.
a) E-mail: nishii@bc.niigata-u.ac.jp

DOI: 10.1093/ietcom/e88–b.6.2268

where the surface S' is located close to the physical surface of the antenna.

P'_{rad} actually represents the power radiated into the surrounding region, whereas P_{rad} is more appropriate for describing the attenuation in the medium. For this reason, the gain based on P_{rad} is used in this study. The directivity of the antenna is then given by

$$D = \frac{4\pi U(r,\theta,\phi)}{P_{\mathrm{rad}}|_{r=r}} = \frac{4\pi U(0,\theta,\phi)}{P_{\mathrm{rad}}|_{r=0}} \tag{3}$$

where $U(r,\theta,\phi) = e^{2\alpha r}U(0,\theta,\phi)$ denotes the radiation intensity at the point (r,θ,ϕ) in spherical coordinates. The absolute gain is then finally given by

$$G = eD = e\frac{4\pi U(r,\theta,\phi)}{P_{\mathrm{rad}}|_{r=r}} = e\frac{4\pi U(0,\theta,\phi)}{P_{\mathrm{rad}}|_{r=0}} \tag{4}$$

where e denotes the radiation efficiency due to condition and dielectric losses. In the following formulation, the distance between two antennas satisfies the far-field criterion for each antenna.

2.2 Principle and Formulation of Measurement

For polarization-matched antennas, the decibel form of the Friis transmission formula in a dissipative medium can be written as

$$10\log_{10}\frac{P_r}{P_t} = -20\log_{10}R - 8.686\alpha R + A, \tag{5}$$

where P_r/P_t is the ratio of the received to transmitted power. A is independent of the distance R, and is given by

$$A = 20\log_{10}\left(\frac{\lambda_e}{4\pi}\right) + (G_t)_{\mathrm{dB}} + (G_r)_{\mathrm{dB}} + 10\log_{10}(1-|\Gamma_t|^2) + 10\log_{10}(1-|\Gamma_r|^2), \tag{6}$$

where λ_e is the equivalent wavelength of the medium, $(G_t)_{\mathrm{dB}}$ and $(G_r)_{\mathrm{dB}}$ are the absolute gains (dB) of the transmitting and receiving antennas, and Γ_t and Γ_r are the reflection coefficients of the transmitting and receiving antennas. When the transmitting and receiving antennas are connected to the ports 1 and 2 of a network analyzer, as shown in Fig. 1, the power ratio of the left-hand side of Eq. (5) is given by

$$|S_{21}|_{\mathrm{dB}} = -20\log_{10}R - 8.686\alpha R + A. \tag{7}$$

Here, α and A can be determined by measuring $|S_{21}|_{\mathrm{dB}}$ as a function of R and fitting the measured data to the curve of Eq. (7) by a least-squares method.

In the following procedure, the sum of absolute gains $(G_t)_{\mathrm{dB}} + (G_r)_{\mathrm{dB}}$ are determined from the constant A. $|\Gamma_t|$, $|\Gamma_r|$ can be obtained by measuring S_{11} and S_{22}. The phase constant of the medium β is obtained by measuring $\angle S_{21}$ as a function of R and fitting the measured data to the straight line given by the following equation:

$$\angle S_{21} = -\beta R + B, \tag{8}$$

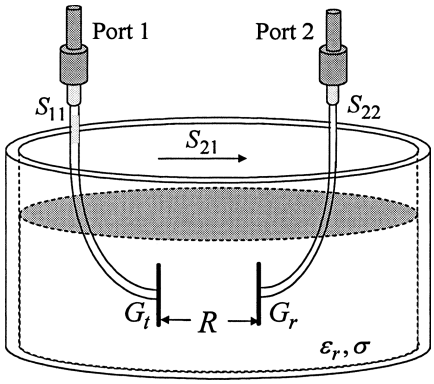

Fig. 1 Transmitting and receiving antennas in solution.

where B is a constant. Then, by definition, the equivalent wavelength is given by

$$\lambda_e = \frac{2\pi}{\beta}. \tag{9}$$

Once $|\Gamma_t|$, $|\Gamma_r|$ and λ_e are known, the sum of absolute gains $(G_t)_{\mathrm{dB}}$ and $(G_r)_{\mathrm{dB}}$ can be determined by

$$(G_t)_{\mathrm{dB}} + (G_r)_{\mathrm{dB}} = A - 20\log_{10}\left(\frac{\lambda_e}{4\pi}\right) - 10\log_{10}(1-|\Gamma_t|^2) - 10\log_{10}(1-|\Gamma_r|^2). \tag{10}$$

The dielectric constant ε_r and conductivity σ of the medium can then be determined as follows.

$$\varepsilon_r = \frac{\beta^2 - \alpha^2}{\omega^2\mu_0\varepsilon_0}, \tag{11}$$

$$\sigma = \frac{2\alpha\beta}{\omega\mu_0}. \tag{12}$$

Here $\omega = 2\pi f$ is the angular frequency (f: frequency), and μ_0 and ε_0 are the permeability and permittivity of free space, respectively.

A three-antenna method [14] based on Eq. (10) is applied to determine the absolute gain of each antenna. The three antennas take three measurements for all combinations of the antennas, and the results are expressed by the following equations:

$$\left.\begin{aligned}(G_1)_{\mathrm{dB}} + (G_2)_{\mathrm{dB}} &= W_A\\ (G_2)_{\mathrm{dB}} + (G_3)_{\mathrm{dB}} &= W_B\\ (G_3)_{\mathrm{dB}} + (G_1)_{\mathrm{dB}} &= W_C\end{aligned}\right\}, \tag{13}$$

where $(G_i)_{\mathrm{dB}}$ denotes the absolute gain of the ith antenna, and W_A, W_B, and W_C are the measured sums of two gains for the combinations 1–2, 2–3, and 3–1, respectively. The gain of each antenna can then be determined by solving the simultaneous Eq. (13).

2.3 Problems in Simultaneous Measurement

A problem occurs when fitting the measured data to the curve given by Eq. (7). The far-field criterion, which was

assumed in deriving the Friis transmission formula, is not satisfied in the region where two antennas are extremely close. Therefore, that data cannot be used for curve-fitting to Eqs. (7) and (8). For a half-wavelength dipole, the maximum dimension of the antenna D_m is equal to $\lambda_e/2$, and the far-field boundary is given by [14]

$$R \geq \frac{|\gamma| D_m^2}{\pi} = \frac{\pi\sqrt{\alpha^2+\beta^2}}{\beta^2}, \tag{14}$$

where $\gamma = \alpha + j\beta$ is the propagation constant of the medium. For example, in the case of deionized water at 32°C, α = 24.0 Np/m and β = 454.5 rad/m at 2.5 GHz [15] such that the measured data for S_{21} in the range $R \geq 6.9$ mm should be used. On the other hand, $|S_{21}|_{\mathrm{dB}}$ decreases below the noise floor of the system and cannot be measured when the distance between two antennas is larger due to the large attenuation in the medium. In practice, the range of R should be limited so as to avoid the logarithmic behavior of the $|S_{21}|_{\mathrm{dB}}$ curve and the noise floor.

Another problem is the phase lapping of $\angle S_{21}$. As the phase displayed on the network analyzer is bounded between $-\pi$ and $+\pi$, the effect of phase lapping in the raw data of $\angle S_{21}$. That is, $\angle S_{21}$ is a linear function of R, but the measured phase data must be fitted to the straight line of Eq. (8).

3. Measurement Setup

3.1 Measurement Setup and Procedure

The measurement setup is outlined in Fig. 2. The bolus tank had a diameter of 900 mm and height of 350 mm, and is filled with 160 l of solution. The transmitting antenna was fixed, while the receiving antenna was moved by a stage-by-stage controller and personal computer (PC). A vector network analyzer (Agilent 8720ES) was used for S parameter measurement.

In measurement, the reference planes of port 1 and 2 were first determined and calibrated. The antennas, with semi-rigid coaxial cable, were connected to the ports and immersed in the solution. For measurement purposes, the antennas are assumed to include the semi-rigid cable. S_{21} was measured in the range of $R = 0 - 150$ mm in increments of 1 mm, S_{11} and S_{22} were measured at $R = 150$ mm to obtain $|\Gamma_t|$ and $|\Gamma_r|$. Although the measured S parameters include the contribution of the semi-rigid cables, no correction is required for electric length because the performance of the antenna with the cable is considered in the design of the fan beam-type CP-MCT scheme.

3.2 Measurement Solutions

Two solutions were examined in the present study: deionized water, and a 0.69% saline solution, both maintained at 32°C. The 0.69% saline solution was used as a bolus to reduce reflections from the target, with dielectric properties almost equivalent to living tissue [4]. An output power of 5 dBm of the network analyzer is fed to the transmitting antenna through the flexible cable with the length of 3.25 m and the attenuation of about 0.3 dB. No amplifiers were used in the present measurements.

3.3 Printed Dipole

The printed dipole used in the measurements is shown in Fig. 3. The dipole was etched on a dielectric slab and the arms of the dipole were soldered to the inner and outer conductors of the semi-rigid coaxial cable. The balun was not used, as the unbalanced current would be degraded. The final dipole had a length of l = 15 mm and width of w = 1 mm, and the dielectric slab had a length of L = 35 mm, width of W = 13 mm, thickness of D = 1 mm, and dielectric constant of 2.2. Figs. 4 and 5 show examples of the return loss of the printed dipoles in deionized water and the 0.69% saline solution. At 2.5 GHz and 32°C, the return loss is −13.3 dB for deionized water and −11.4 dB for the 0.69% saline solution. The antennas were physically supported by the long semi-rigid coaxial cables, and fishing line was used to link the antenna to the stage to avoid reflections from a jig or other device.

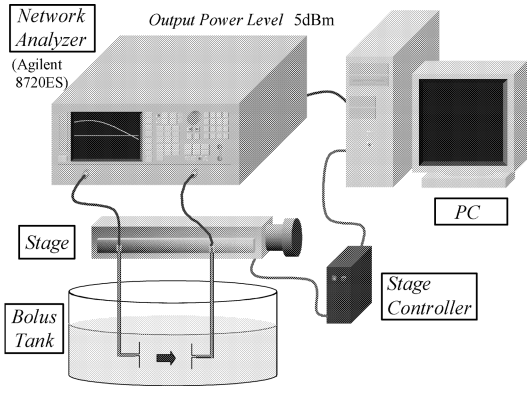

Fig. 2 Measurement setup.

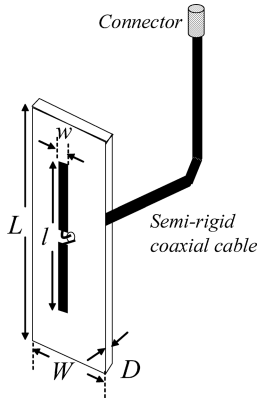

Fig. 3 Printed dipole.

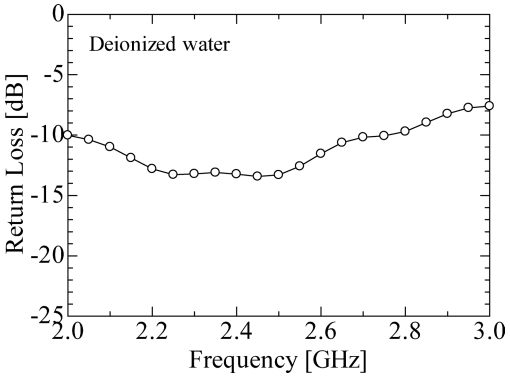

Fig. 4 Return loss of printed dipole in deionized water.

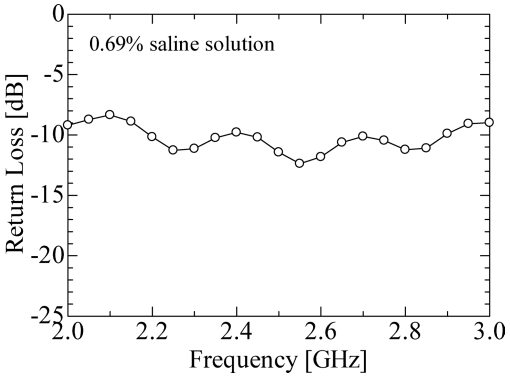

Fig. 5 Return loss of printed dipole in 0.69% saline solution.

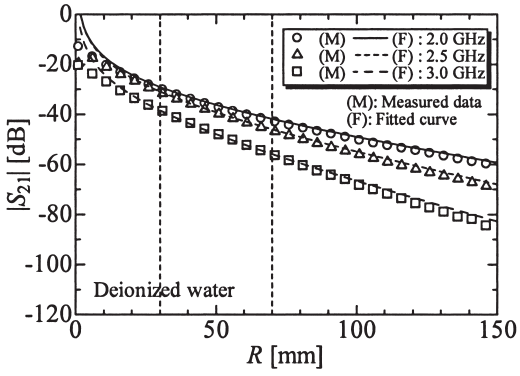

(a) $|S_{21}|_{\mathrm{dB}}$

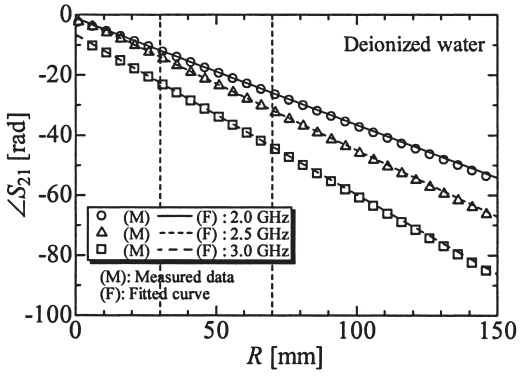

(b) $\angle S_{21}$

Fig. 6 Curve fitting for deionized water.

4. Results

4.1 Curve-Fitting for $|S_{21}|_{\mathrm{dB}}$ and $\angle S_{21}$

The regression curves for the attenuation and phase constants were determined by fitting Eqs. (7) and (8) to the measured values of $|S_{21}|_{\mathrm{dB}}$ and $\angle S_{21}$, respectively. The measured data and corresponding curves for deionized water and the 0.69% saline solution are shown in Figs. 6 and 7. The range of fitting is 30 mm $\leq R \leq$ 70 mm for both solutions (dotted lines in the figures). The figures show one of three curves obtained for the three combinations at each frequency. The curves for the other combinations are almost identical to the curves shown in Figs. 6 and 7.

As can be seen in the figures, the measured values of $|S_{21}|_{\mathrm{dB}}$ tend to deviate from the regression curves in the range of low R ($\leq$ 15 mm), where the contribution of the $1/R^2$ and $1/R^3$ terms of the electric field of the transmitting antenna cannot be ignored. This problem arises from the far-field approximation in Eq. (5) and as such the data measured in the extreme near-field region should be excluded in the fitting process. Irregular behavior of $|S_{21}|_{\mathrm{dB}}$ and $\angle S_{21}$ also occurs in the saline solution at large R ($\geq$ 100 mm). This can be attributed to the larger attenuation at longer distance. The attenuation constant of the solution also increases with frequency such that the measured field is below the noise floor, -100 dB in the present measurements. It should be noted that some of the data for $\angle S_{21}$ are out of phase with the regression line by $\beta R = 2n\pi$ (n: integer) due to incomplete phase lapping correction. Thus, if the range of the fitting is appropriately selected, valid curves can be obtained. That is, the attenuation and phase constants, and the sum of the gains can be obtained as a function of the frequency.

4.2 Dielectric Properties of Solutions

The estimated attenuation and phase constants are shown in Figs. 8 and 9 for deionized water and the 0.69% saline solution, with empirical curve [15] shown for reference. Although the phase constant of the saline solution is the same as that of deionized water, the attenuation constant of the saline solution is markedly different. For example, α = 198 dB/m for deionized water, while α = 473 dB/m for the 0.69% saline solution at 2.5 GHz. This difference gives rise to the problem related to the noise floor.

The estimated dielectric constant and conductivity of the solutions are shown in Figs. 10 and 11, with empirical curves [15] for reference. Although slight differences between the measured and empirical curves can be observed, the figures demonstrate the validity of this simultaneous measurement technique for estimation of the dielectric properties of the solution.

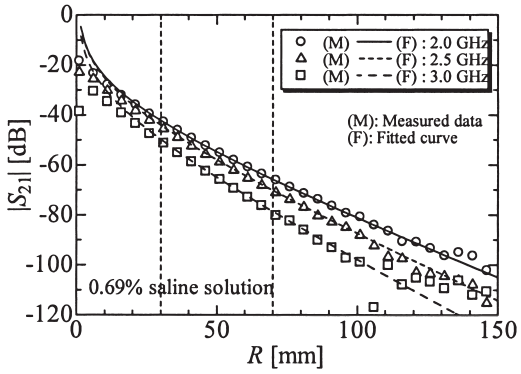

(a) $|S_{21}|_{\mathrm{dB}}$

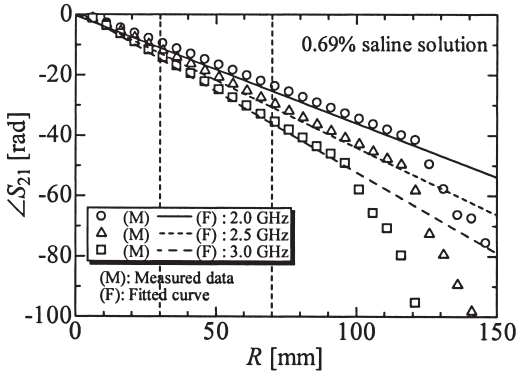

(b) $\angle S_{21}$

Fig. 7 Curve fitting for 0.69% saline solution.

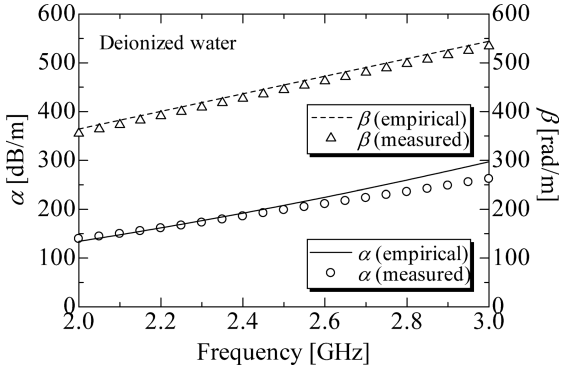

Fig. 8 Attenuation and phase constants of deionized water.

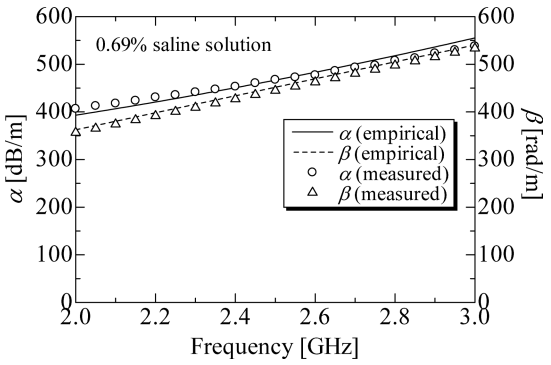

Fig. 9 Attenuation and phase constants of 0.69% saline solution.

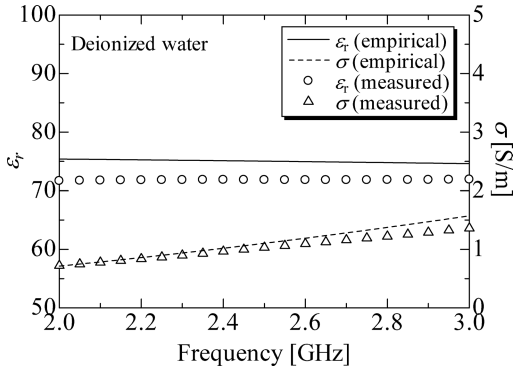

Fig. 10 Dielectric constant and conductivity of deionized water.

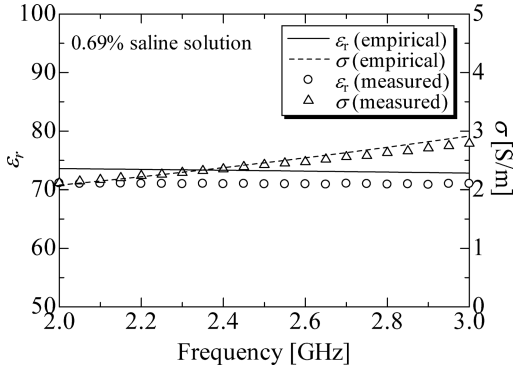

Fig. 11 Dielectric constant and conductivity of 0.69% saline solution.

4.3 Absolute Gain of Printed Dipoles

Figures 12 and 13 show the estimated absolute gains of three printed dipoles in deionized water and the 0.69% saline solution. The absolute gains are relatively uniform, with mean values of 1.9 dBi and −0.1 dBi in deionized water and the 0.69% saline solution at 2.5 GHz. Approximate gains can also be calculated using Richmond's code [16]. For a thin dipole with length of 15 mm and diameter of 1 mm, the gains at 2.5 GHz are 2.05 dBi and 0.05 dBi for deionized water and the 0.69% saline solution, respectively. The largest difference among the three measured gains is about 0.5 dB, and the measured gains are in good agreement with calculated results within ±0.2 dB. The error in the gain is therefore considered to be less than 0.5 dB, which also demonstrates the validity of this gain measurement technique.

The gains in saline solution are smaller those in deionized water. Equation (1) shows that near-field loss can be severe generally increasing with the conductivity of the medium [9]. The difference between the measured and calculated gains can be attributed to a number of factors. The difference of 0.2 dB is considered to be mainly due to losses at the connection, in the semi-rigid cable, and soldering.

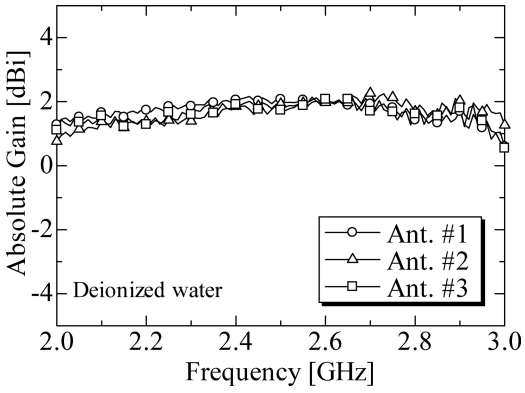

Fig. 12 Absolute gain of printed dipole in deionized water.

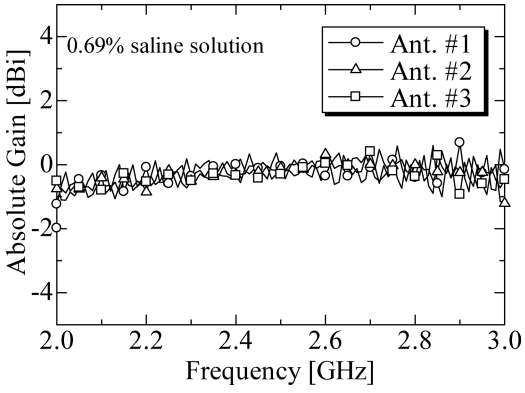

Fig. 13 Absolute gain of printed dipole in 0.69% saline solution.

The antennas will also exhibit slight differences from one another as the antennas were all hand-made. As the attenuation becomes larger, the constant A in Eq. (5) becomes smaller. That is, A is sensitive to the distance, R. Thus, if the attenuation constant is correctly estimated, the change in gain will be approximately ± 0.24 dB for ± 1 mm change in the distance at 2.5 GHz in the 0.69% saline solution. This effect may appear in the results when a pair of printed dipoles is slightly misaligned. Furthermore, the distance may not be determined exactly because the center of the antenna was not accurately calibrated. Finally, if the error related to the reflection coefficient of the antenna is $\pm 5\%$, the gain will have error of about 0.1 dB according to Eq. (10). For example, RL = -13.3 dB. However, this effect is considered to be negligible.

5. Conclusion

A method for simultaneously measuring the absolute gain of an antenna in solution and the dielectric properties of the solution was proposed. The method is a three-antenna method based on modified Friis transmission formula with curve-fitting. The measured absolute gains of printed dipole antennas in solution are in good agreement with the calculated results, demonstrating the validity of the method.

References

[1] J.H. Jacobi and L.E. Larsen, "Microwave time delay spectroscopic imagery of isolated canine kidney," Med. Phys., vol.7, no.1, pp.1–7, 1980.
[2] L.E. Larsen and J.H. Jacobi, Medical applications of microwave imaging, IEEE Press, 1986.
[3] M. Miyakawa, "An attempt of microwave imaging of the human body by the chirp radar-type microwave CT," IEICE Trans. Inf. & Syst. (Japanese Edition), vol.J75-D-II, no.8, pp.1447–1454, 1992.
[4] M. Miyakawa and J.C. Bolomey, Non-invasive thermometry of the human body, pp.105–126, CRC Press, 1996.
[5] M. Miyakawa, E. Harada, and W. Jing, "Chirp pulse microwave computed tomography (CP-MCT) equipped with a fan beam scanner for high-speed imaging of a biological target," Proc. 25th Ann. Int. Conf. Eng. in Medicine and Biology Society, pp.1031–1034, 2003.
[6] R.W.P. King and G.S. Smith, Antennas in matter, MIT Press, 1981.
[7] H.R. Underwood, A.F. Peterson, and R.L. Magin, "Electric-field distribution near rectangular microstrip radiators for hyperthermia heating: Theory versus experiment in water," IEEE Trans. Biomed. Eng., vol.39, no.2, pp.146–153, 1992.
[8] C.K.H. Tsao and R. Co, "Radiation resistance of antennas in lossy media," IEEE Trans. Antennas Propag., vol.AP-19, no.3, pp.443–444, 1971.
[9] J.H. Richmond, "Radiation and scattering by thin-wire structures in the complex frequency domain," NASA Report, CR-2396, 1974.
[10] L.N. Ahlonsou, C. Grangeat, C. Person, and F.L. Pennec, "Calibration of SAR probes at mobile phones frequencies," Proc. 26th General Assembly URSI, p.847, 1999.
[11] D. Misra, M. Chabbra, B.R. Epstein, M. Mirotznik, and K.R. Foster, "Noninvarsive electrical characterization of materials at microwave frequencies using an open-ended coaxial line: Test of an improved calibration technique," IEEE Trans. Microw. Theory Tech., vol.38, no.1, pp.8–14, 1990.
[12] C.K. Chou, G.W. Chen, A.W. Guy, and K.H. Luk, "Formulas for preparing phantom muscle tissue at verious radiofrequencies," Bioelectromagnetics, vol.5, pp.435–441, 1984.
[13] A. Toropainen, P. Vainikainen, and A. Drossos, "Method for accurate measurement of complex permittivity of tissue equivalent liquids," Electron. Lett., vol.36, no.1, pp.32–34, 2000.
[14] C.A. Balanis, Antenna theory: Analysis and design, 2nd ed., John Wiley & Sons, 1997.
[15] K. Magario and I. Yamaura, "Temperature dependence of microwave dielectric properties in saline solution," IEICE Technical Report, EMCJ88-11, 1988.
[16] J.H. Richmond, "Computer program for thin-wire structure in a homogeneous conducting medium," NASA Report, CR-2399, 1974.

Nozomu Ishii was born in Sapporo, Japan, in 1966. He received the B.S., M.S., and Ph.D. degrees from Hokkaido University, Sapporo, Japan, in 1989, 1991, and 1996, respectively. In 1991, he joined the faculty of Engineering at Hokkaido University. Since 1998, he has been with the faculty of Engineering at Niigata University, Japan, where he is currently an Associate Professor of the Department of the Biocybernetics. His current interests are in the area of small antenna, planar antenna, millimeter antenna, antenna analysis, antenna measurement, and electromagnetic compatibility. He is a member of the IEEE.

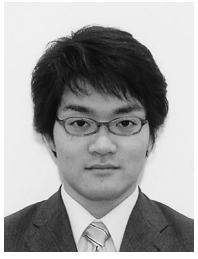

Yoshikazu Yonemura was born in Kobe, Japan, in 1980. He received the B.S. and M.S. degrees from Niigata University, Niigata, Japan, in 2002 and 2004, respectively. He is currently a student of the Graduate School of Science and Technology, Niigata University. His research interests include gain measurement in the solution.

Michio Miyakawa was born in Gunma Prefecture, Japan, in 1947. He received D. Eng. degree from Hokkaido University, Sapporo, Japan, in 1977. He joined the Electrotechnical Laboratory, Japanese Agency of Industrial Science and Technology (AIST), MITI, Tsukuba, Japan, in 1977, where he became a Senior Research Scientist in 1982 and worked on infrared- or microwave-thermometry in addition to organizing the National Project by MITI on the development of hyperthermia equipment for cancer treatment. In 1991, he was appointed Professor at Faculty of Engineering, Niigata University, Niigata, Japan, where he has been involved in research programs relating to noninvasive thermometry using microwaves, methods of three-dimensional local SAR measurement and observation, themes on human interface, and so on. Currently, he is a Professor of the Center for Transdisciplinary Research at the university. From 1995 to 1996, has was a Visiting Scientist at the Central Institute for Biomedical Engineering, University of Ulm, Ulm, Germany, where he was involved in research project for developing the hyperthemia system. Dr. Miyakawa is a member of the IEEE, IEE of Japan, Japanese Society of ME and BE, Information Processing Society of Japan, Society of Instrument and Control Engineers, and Japanese Society of Hyperthermic Oncology.